PHYSICAL REVIEW
LETTERS

VOLUME 44 | 17 MARCH 1980 | NUMBER 11

Direct Measurement of the Velocity Autocorrelation Function for a Brownian Test Particle

Paul D. Fedele and Yong W. Kim
Department of Physics, Lehigh University, Bethlehem, Pennsylvania 18015
(Received 5 November 1979)

The velocity autocorrelation function is measured directly for the first time for one Brownian test particle in nitrogen at two different densities. The persistence of the autocorrelation is more pronounced than predicted on the basis of the modified Langevin equation. The measured distribution for the Brownian displacement shows a considerable departure from the Gaussian distribution at both densities.

The 1967 discovery by Alder and Wainwright of the slowly decaying nonexponential tail of the velocity autocorrelation function of hard-sphere molecules as revealed in molecular-dynamics computations has led to a flurry of theoretical activities.[1] On one hand, correlated binary collisions or ring events have been established as the reason for this apparently non-Markovian behavior, and basic reformulation of the kinetic equations has been effected by means of the ring diagrams. On the other hand, the persistence of the autocorrelation has been attributed to the hydrodynamic modes of the fluctuating flow field around the test molecule. The successful derivation of the Stokes law as well as the Basset-Boussinesq correction term by means of the repeated ring events[2] points to certain compatibility between the two viewpoints. In this Letter we present the first directly measured Brownian velocity autocorrelation function from a new experiment, which has been in the making since 1975.[3]

It has been implied that the developments in the molecular fluctuations hold for the Brownian motion except for parametric differences. The success with the modified Langevin equation supports this notion[4]:

$$m\frac{d\vec{v}}{dt} = -\xi(\rho,R)\vec{v} - \frac{2\pi}{3}\rho R^3\frac{d\vec{v}}{dt} - 6R^2(\pi\rho\eta)^{1/2}\int_{-\infty}^{t}\frac{d\vec{v}}{ds}(t-s)^{-1/2}ds + \vec{f}(t), \tag{1}$$

where the Stokes-Cunningham coefficient $\xi(\rho,R)$ becomes $6\pi\eta R$ (stick) or $4\pi\eta R$ (slip). The notations of Ref. 4 are used for other symbols.

The situation is quite different in the (laboratory) experimental front. The first[4] of the four reported experiments consisted of testing the validity of Eq. (1) through exploitation of the limiting behavior of Eq. (1). While the result was found consistent with Eq. (1), including the $(\text{time})^{-3/2}$ tail, it is unsatisfactory to examine such a fundamental phenomenon with data requiring interpretation through the phenomenological Eq. (1). In the three other experiments,[5] consequences of the Alder-Wainwright effect in transport properties had been searched for. Results indicated certain nonclassical behavior of the velocity autocorrelation function but failed to give details as to the exact nature of the behavior. We note that in these approaches it is not possible to measure the function directly and independently.

The experiment has proven to be difficult but the experimental approach is straightforward:

We suspend a single Brownian particle in a cell containing a gas and measure a horizontal component of the Brownian velocity successively in order to construct the autocorrelation function. The velocity component is determined by measuring the displacement of the magnified image of the particle during a time interval which is smaller than the characteristic relaxation time of the test particle in the host medium. The displacement is obtained from the change in the total intensity of the particle image transmitted through a neutral-density wedge filter situated at the image plane.

Figure 1 shows details of the Brownian cell and the high-pressure vessel. Particles in the settling chamber are let into the cell by sedimentation. The single test particle selected in the next hour or so is retained for measurements at different densities for up to 15 h by continuous surveillance with three video cameras. The density of the gas is varied by changing the pressure in the vessel. The rate of pressurization depends on the extent to which the test particle can be controlled by the electric field and has been in the range of 2 to 5 atm/h thus far. After a desired pressure is reached, the test particle is moved about in the cell in order to ascertain full decay of eddies created in the gas by pressurization before starting the measurement. The measured long-term leak rate of the vessel is considerably less than 2×10^{-4} Torr/sec at 20 atm.

The particle-position data are taken in files of 2019 points each at the rate of 20 MHz and this means that the test-particle velocity, as approximated by the displacement during 50 nsec is obtained independently once every 100 nsec. In each run, typically 1000 such files of data are taken and stored in a PDP-11/34A minicomputer.

Because of the limited photon flux and even smaller photoelectron count rate, the position detector output consists of high-frequency, large-amplitude (rather than expected small-amplitude) fluctuations superimposed on a low-frequency background signal corresponding to large-time-interval displacements. The net result of this apparent or pseudo noise introduced in the data is to make the small-time displacements very large and introduce a negative autocorrelation at times comparable to half the periods of the high-frequency pseudonoise part.

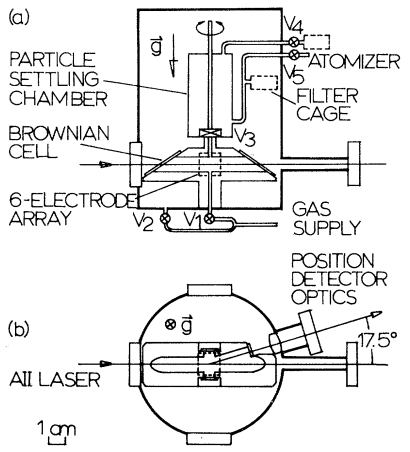

FIG. 1. High-pressure vessel containing the Brownian cell and particle-settling chamber: (a) a side view and (b) a top view. Various components within the vessel normally experience no pressure gradient. During the period of data collection, the Brownian cell of 3 cm^3 in volume is sealed vacuum tight and all six electrodes are grounded to the cell body.

The final method adapted to overcome this difficulty is to apply a q-point running average on each N-point data file to end up with an $(N-q)$-point data file before processing the full run. For values of q such that $q\delta T$ is large in comparison with the pseudonoise periods, where δT is the time between two successive position measurements, the pseudonoise contributions average out to an addititive constant. The velocity is then actually an average of two Brownian velocities separated in time by $q\delta T$, and a typical term appearing in the sum for computation of the autocorrelation function is as follows:

$$\tfrac{1}{4}[v(T)+v(T+q\delta T)][v(T+t)+v(T+q\delta T+t)]$$
$$=\tfrac{1}{4}[v(T)v(T+t)+v(T+q\delta T)v(T+q\delta T+t)+v(T+q\delta T)v(T+t)+v(T)v(T+q\delta T+t)], \quad (2)$$

where T is the laboratory time of measurement and t the correlation time. Upon taking of an ensemble average, the first two terms on the right-hand side become identical, giving rise to the value of the autocorrelation function at t. The last two terms also become identical to each other but vanishingly small in comparison to the first two because $q\delta T$ is generally much larger than the range of t considered here.

The above conclusions are exact in the limit of $N\to\infty$. Extensive numerical simulation using

randomly generated numbers bears out all of the conclusions. The situation is somewhat different for the actual experiment in that $N = 2019$ in each file. Both the experimental uncertainty and long-time correlation increase as q exceeds significantly a certain range. In other words, there is no sharply defined criterion for choosing the length of the running-average interval, although a plausible range is identifiable.

In order to overcome the ambiguity associated with the running-average technique under the finite sample-size condition, measurements are made for each test particle at two different gas densities. The run under the standard gas condition is first processed to find an optimum q value (q_0) such that the resulting velocity autocorrelation function best fits the solution of Eq. (1). The higher-density run is then analyzed using the q_0-point running average and the result compared with the solution of Eq. (1) at that density.

Two sets of measurements for one Brownian test particle, consisting of four runs each at two different densities of nitrogen, are summarized in Fig. 2. Each run consists of approximately 1.8 million position measurements. The four resulting velocity autocorrelation functions at each of the two densities have been averaged and the average is plotted as a function of the dimensionless time t/τ_p, where τ_p is obtained by best fitting the short-time portion of each autocorrelation function (either theoretical or measured) with $\exp(-t/\tau_p)$. A running average of $q_0 = 125$ has been performed in each run.

There is a systematic discrepancy between the measurement at 1 atm and the theory for $t \gtrsim 3.5\tau_p$ in spite of an effort to optimize the fit. The discrepancy does not seem accidental: Firstly, a similar trend is seen at the higher-density run. Secondly, when one examines $\rho_D(t)$ as the solution of Eq. (1) in the long-time regime, it displays the asymptotic $(t/\tau_p)^{-3/2}$ tail by breaking away from the intermediate-time trend in the manner rather similar to this. Thirdly, the measurement at the higher density indeed shows the deviation taking place earlier in t/τ_p than

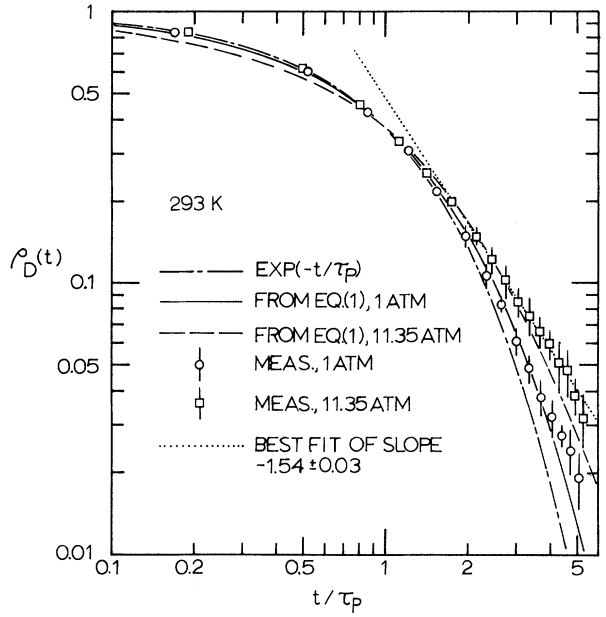

FIG. 2. Normalized velocity autocorrelation function $[\rho_D(t)]$ of a Brownian test particle in nitrogen at two densities as a function of the dimensionless time t/τ_p. Measurements (circles and squares) are compared with the solution of Eq. (1) [see Eq. (3i) of the first paper in Ref. 4]. A power-law fit (dotted line) to the higher-density data reveals the earlier-than-expected appearance of the asymptotic behavior. The indicated experimental uncertainty is determined by the point-by-point mean diviation among four runs. This is considerably larger than the combined systematic error from laser heating and convection due to pressurization, as judged from the measurements under varying conditions of the laser intensity and post-pressurization waiting time. The systematic error due to the measured leak rate is less than 10^{-3} in $\rho_D(t)$.

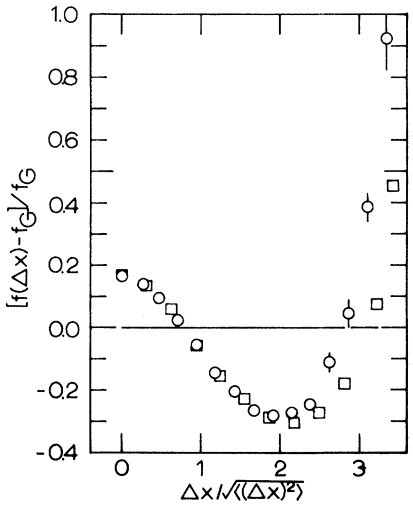

FIG. 3. The distribution of the measured Brownian displacement during δT, relative to the Gaussian distribution, f_G, as a function of the dimensionless displacement $\Delta x/\langle \Delta x^2\rangle^{1/2}$. Results from the same data used in Fig. 2 are shown. About 0.9 million displacements are used to obtain the distribution at each of the two densities: 1 atm (circles) and 11.35 atm (squares) at 293 K.

the atmospheric-pressure measurement, as predicted by the theory.

In Fig. 3 we show the distribution of the x component of the Brownian "velocity" (i.e., displacement Δx during δT), from two of the eight runs used to obtain the results in Fig. 2. In both cases, the distribution is narrower near the center and wider in the wings than the Gaussian. This feature is in qualitative agreement with an earlier *ad hoc* prediction.[6] A similar behavior has been seen in a recent two-dimensional molecular-dynamics computation for a Lorentz gas.[7] In the wings, the measured distribution intersects the Gaussian at different places depending on the density.

We note that the Brownian "velocities" are undetermined to a constant factor as a result of the running-average procedure itself. Also it has not been possible to measure the particle radius independently and accurately because the radius is considerably smaller than the practical wavelength range of light and the Brownian motion is very strong. However, the following estimates point to a degree of self-consistency between observations. The mean square displacement (from the data of Fig. 3) has been observed to decrease with increasing density. The measured ratio of the 11.35-atm over 1-atm value is 0.59, which gives the particle radius of 0.11 μm according to the Millikan rule.[8] From the particle relaxation time of the 1-atm runs, one obtains an estimate of 0.10 ± 0.01 μm. The sedimentation velocity gives another estimate for the radius of 0.11 ± 0.015.

Our measurement shows that the Alder-Wainwright effect is overall more pronounced than thought possible for the Brownian motion. The exact reasons for the observation, particularly the early appearance of the asymptotic tail, are not understood.

We thank Professor J. A. McLennan, Professor R. J. Emrich, Professor J. R. Dorfman, and Professor E. G. D. Cohen for helpful discussions and Dr. J. C. Modla for contributions to early phases of this work. The financial support of the National Science Foundation (Grants No. PHY-79-09267 and No. PHY 77-07858) and the Pennsylvania Power and Light Company is gratefully acknowledged. One of us (P.D.F.) was a recipient of a Gotshall Graduate Fellowship.

[1]See references in J. C. Modla, Ph.D. thesis, Lehigh University, 1977 (unpublished); Y. W. Kim and J. C. Modla, Bull. Am. Phys. Soc. 22, 1283 (1977); Y. W. Kim and J. E. Matta, Phys. Rev. Lett. 31, 208 (1973), and in *Recent Development in Shock Tube Research*, edited by D. Bershader and W. Griffith (Stanford Univ. Press, Stanford, 1973); J. E. Matta, Ph.D. thesis, Lehigh University, 1974 (unpublished); J. P. Boon and A. Bouiller, Phys. Lett. 55A, 391 (1976); J. DeZwaan and Y. Yonas, J. Chem. Phys. 63, 4606 (1975); J. T. Hynes, R. Kapral, and M. Weinberg, J. Chem. Phys. 69, 2725 (1978); S. H. Chen, T. A. Postal, and K. Sköld, Phys. Rev. A 16, 2112 (1977).

[2]J. R. Dorfman, H. van Beijeren, and C. F. McLure, in *Proceedings of the Symposium on Continuum Models of Discrete Systems* (Polish Academy of Sciences, Warsaw, 1975); J. R. Dorfman, private communication.

[3]Modla, Ref. 1; Kim and Modla, Ref. 1.

[4]Kim and Matta, Ref. 1; Matta, Ref. 1.

[5]Boon and Bouiller, Ref. 1; DeZwaan and Yonas, Ref. 1; Hynes, Kapral, and Weinberg, Ref. 1; Chen, Postal, and Sköld, Ref. 1.

[6]J. W. Dufty and J. A. McLennan, Phys. Rev. A 9, 1266 (1974).

[7]W. E. Alley and B. J. Alder, Phys. Rev. Lett. 43, 653 (1979).

[8]R. A. Millikan, Phys. Rev. 22, 1 (1923).